Urban Climate 68 (2026) 103067

Contents lists available at ScienceDirect

Urban Climate

journal homepage: www.elsevier.com/locate/uclim

Spatial spillover effects of German clinker production on regional air pollution

Nargiz Ahmadova [a], Imke Rhoden [a,b,c,*], Stefan Vögele [a,c], Jochen Linßen [a]

[a] Forschungszentrum Jülich GmbH, Institute of Climate and Energy Systems, Jülich Systems Analysis, Wilhelm-Johnen-Str., 52425 Jülich, Germany
[b] Center for Environmental Management, Resources and Energy (CURE), Faculty of Economics, Ruhr-Universität Bochum, Universitätsstr. 150, 44801 Bochum, Germany
[c] Chair of Environmental and Resource Economics, TU Bergakademie Freiberg, Schloßplatz 1, 09596 Freiberg, Germany

ARTICLE INFO

Keywords:
Clinker production
Air pollution
Nitrogen dioxide (NO_2)
Spatial spillover effects
Spatial Durbin model

ABSTRACT

The cement industry is a primary contributor to industrial air pollution, with clinker production representing the most emissions-intensive stage of manufacturing. In Germany, clinker production accounts for approximately 21.1% of total industrial nitrogen oxide emissions, yet its spatial dynamics remain under-researched. This study investigates the direct and spatial spillover effects of clinker production on nitrogen dioxide concentrations across 393 administrative districts from 2018 to 2022. Using a spatial Durbin model to account for regional dependencies, the results reveal that clinker production significantly increases nitrogen dioxide levels. Crucially, the findings indicate that spatial spillover effects on neighboring regions (0.021%) are more than four times larger than direct local impacts (0.005%). These results, which are statistically significant, meaning they differ from random noise, remain consistent across various robustness checks and confirm the presence of significant regional environmental externalities. The study suggests that effective mitigation of nitrogen oxides in Germany requires a shift from localized targets toward coordinated, multi-regional governance frameworks to internalize the transboundary costs of industrial pollution.

1. Introduction

Air pollution represents one of the most pressing environmental challenges of the century, with industrial emissions being a significant contributor. Among industrial sectors, the cement industry is recognized as a primary source of air pollution, contributing substantially to emissions of nitrogen oxides (NO_X), sulfur oxides (SO_X), and dust (Nwogu et al., 2025). In cement manufacturing, clinker-producing factories emit substantially higher primary air pollutants into the atmosphere than their non-clinker-producing counterparts (Firdissa et al., 2024). In Germany, there are 53 cement plants, of which 33 are involved in clinker production (VDZ, 2025). In 2022, these facilities generated approximately 32.9 million tonnes of cement and 23.2 million tonnes of clinker (VDZ, 2023). NO_X has the highest emission factor among pollutants released during clinker production, with approximately 0.5 kg emitted per ton of clinker (German Environment Agency, 2022). This corresponds to approximately 11.6 kt (kilotonnes) of NO_X emitted from clinker production in 2022. Considering Germany's total industrial NO_X emissions of 54.91 kt in 2022 (German

* Corresponding author at: Forschungszentrum Jülich GmbH, Institute of Climate and Energy Systems, Jülich Systems Analysis, Wilhelm-Johnen-Str., 52425 Jülich, Germany.

E-mail address: i.rhoden@fz-juelich.de (I. Rhoden).

https://doi.org/10.1016/j.uclim.2026.103067
Received 23 March 2026; Received in revised form 12 July 2026; Accepted 19 July 2026
Available online 25 July 2026
2212-0955/

Abbreviations

AIC	Akaike Information Criterion
asinh	Inverse hyperbolic sine transformation
BIC	Bayesian Information Criterion
CO_2	Carbon Dioxide
DE	Direct Effect
EKC	Environmental Kuznets Curve
FE	Fixed Effects
GDP	Gross Domestic Product
IE	Indirect (spillover) Effect
kt	Kilotonnes
LR	Likelihood Ratio
NO_2	Nitrogen Dioxide
NO_x	Nitrogen Oxides
NUTS	Nomenclature of Territorial Units for Statistics
OPC	Ordinary Portland Cement
$PM_{2.5}$	Particulate Matter ($\leq$ 2.5 μm diameter)
R&D	Research and Development
SAR	Spatial Autoregressive Model
SDM	Spatial Durbin Model
SDEM	Spatial Durbin Error Model
SEM	Spatial Error Model
SLM	Spatial Lag Model
SO_x	Sulfur Oxides
TE	Total Effect
W1	Queen contiguity spatial weight matrix
W2	Inverse distance spatial weight matrix

Symbol

i	County (NUTS-3 region) index
t	Year index
N	Number of regions (393 in main model; 293 in restricted sample)
K	Number of regressors
a_0	Intercept
β_1–β_{10}	Regression coefficients for explanatory variables
ρ (rho)	Spatial autoregressive coefficient (SDM, SAR)
λ (lambda)	Spatial error coefficient (SEM, SDEM)
θ	Coefficient vector for spatially lagged regressors (spillover effects)
W	Spatial weight matrix (N × N)
W_i	i-th row of W
w_{ij}	Element of W; positive if regions i and j are neighbors, zero otherwise
X_t	N×(K − 1) matrix of control variables for year t
W·X / Wlag.	Spatially lagged explanatory variables
u_{it}	Composite error term
ε_{it}	Idiosyncratic error (SDEM only)
d	Centroid-to-centroid distance between regions (used in W2: weight = 1/d)
σ^2	Residual variance (reported as Sigma2)
Poll	Average NO_2 concentration
Clinker	Clinker production, derived from CO_2 plant emissions
Y	GDP per capita (base year 2010)
Pop	Population density
Ind	Industrial value added as share of total value added
Car	Petrol and diesel passenger cars
Traf	Total road traffic accidents
Rd	Employees in knowledge- and research-intensive industries
RenH	Newly completed residential buildings with renewable heating
Wind	Average yearly wind speed

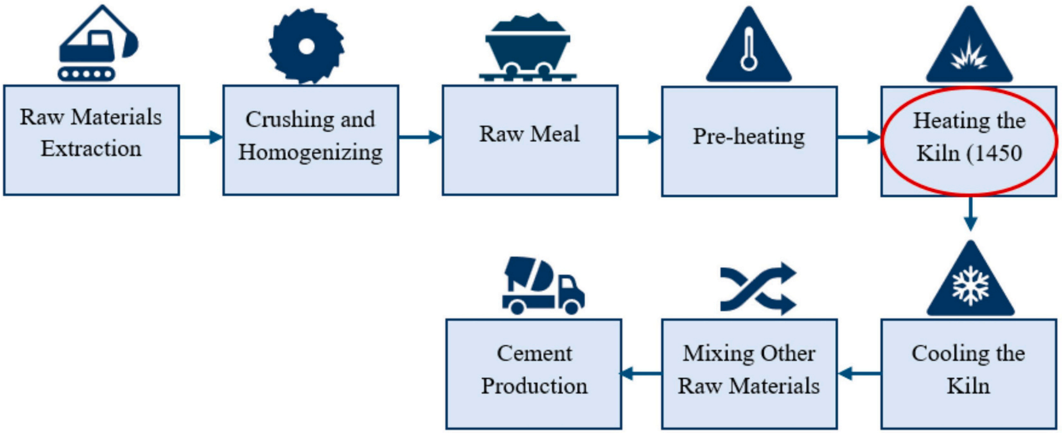

Fig. 1. Cement production process flow. Source: Own illustration (Cembureau, 2017).

Environment Agency, 2025), the clinker sector alone accounted for approximately 21.1%. These figures underscore the importance of examining the contribution of clinker production to air pollution in Germany.

Emissions from clinker plants not only affect the host area but also spill over into adjacent regions. This phenomenon is traditionally assessed using atmospheric dispersion models, such as the ExternE "Impact Pathway" methodology, which calculates pollutant flows based on meteorological data (wind speed and direction, precipitation), stack height, and technical siting (Bickel et al., 2005, Sustainability Directory, 2024). While highly precise for tracking primary particles, these models are essentially deterministic and physical, focusing on the end-of-pipe transport of molecules.

This paper addresses the spread of emissions by offering a distinct research contribution by shifting the focus from physical dispersion to economic spatial dependence. Unlike dispersion models, a spatial econometric approach captures the aggregate regional externality. This includes not only the physical drift of NO_X but also the induced co-effects associated with clinker production, such as intensified heavy-duty logistics, supply chain activity, and secondary economic impacts, which are typically outside the scope of meteorological models. Employing a spatial Durbin model (SDM) provides a holistic alternative that quantifies how industrial hubs function as spatial drivers of pollution across administrative boundaries. Empirical research also supports this spatial interdependence, confirming the spatial autocorrelation of air pollutants (Dai and Zhou, 2017; Wu et al., 2022). These studies suggest that pollution levels in one region are not independent of those in neighboring areas. Therefore, this paper examines both the direct impact of clinker production on air quality and its spatial spillover effects across 393 NUTS-3-level (nomenclature of territorial units for statistics) regions in Germany.

The remainder of this paper is structured as follows: Section 2 reviews the existing literature and describes the characteristics of clinker production and its associated pollution. Section 3 presents the data and methodology; Section 4 illustrates and discusses the results. Section 5 concludes with policy implications.

2. Clinker production and air pollution

The research on the cross-regional pollution effects of clinker production remains relatively scarce. A closely related contribution is Li et al. (2020), which examines the spatial spillover effects of cement production on air pollution in China using a panel data set of 30 provinces. The authors use PM2.5 concentrations as a measure of air pollution and macroeconomic socioeconomic factors (e.g., economic growth, industrial structure, transportation intensity) as explanatory variables.

While research on clinker-related pollution spillovers is limited, the literature has established spatial spillover effects in other contexts. For instance, Zhao and Wang (2022) and Ding and Liu (2023) examine how a region's level of urbanization influences pollution both locally and in adjacent regions. Li et al. (2018) study the spatial spillover effects of industrialization and urbanization on seven types of pollutant emissions across 53 cities in China's Huang-Huai-Hai region. Feng et al. (2020) investigate the effect of environmental regulations on the surrounding regions, while Ma et al. (2016) examine how economic activities (e.g., industrial production, urbanization, transportation, energy use) contribute to PM2.5 pollution in nearby regions. These studies collectively provide empirical evidence of significant spatial spillover effects.

This study contributes to the literature in several ways. First, no existing research has examined the spatial spillover effects of cement or clinker production on air pollution in Germany; this study therefore addresses this gap. Second, only a limited number of studies have investigated such effects at a micro-regional scale comparable to NUTS-3. In addition, existing studies mostly focus on regional socioeconomic drivers of air pollution. However, this study also incorporates wind speed as a key meteorological factor influencing the dispersion of air pollutants.

2.1. Clinker production within the cement manufacturing process

All over the world, cement is a critical component for the construction sector. The primary raw materials for making cement are limestone, clay, and marl (European Environment Agency, 2023). The description refers to the production of Ordinary Portland Cement (OPC), the standard cement type worldwide. Other cement types may involve variations in raw materials or processing steps. Firstly, these ingredients are crushed and blended to form the raw meal (see Fig. 1). The raw meal is then fed into a preheater tower, where it is heated before entering the kiln. In the final stage, the raw meal is heated at around 1450 °C, a process called calcination. During calcination, limestone (calcium carbonate) decomposes into lime (calcium oxide) at high heat, and this lime then combines with other raw materials to form clinker. After cooling, the clinker is ground with gypsum and other additives to produce cement.

As the primary component of cement, clinker is the main source of pollution in cement manufacturing. As marked with a red circle in Fig. 1, the kiln heating stage for clinker formation represents the most emission-intensive step in the process. The extremely high temperatures needed to produce clinkers cause physical and chemical reactions of raw materials and fuels, which in turn release significant amounts of emissions into the atmosphere. NO_X is the main pollutant emitted from the kiln, followed by SO_X, dust, and volatile organic compounds (European Environment Agency, 2023). However, since most nitrogen monoxides are converted into nitrogen dioxide (NO_2) in the atmosphere, local emission data are reported as NO_2 per cubic meter (VDZ, 2023). Accordingly, to be consistent with the available data, this paper uses NO_2 concentrations as the measure of air pollution.

2.2. Spatial distribution of air pollution in Germany

NO_2 is a significant air pollutant that poses serious risks to both human health and the environment. The main sources of this pollutant are road transport and combustion processes in industry and energy supply (European Environment Agency, 2025). Exposure has been linked to various diseases, including lung function impairment (Jiang et al., 2019) and an increased risk of mortality from pulmonary heart disease (Chen et al., 2019).

Fig. 2a shows a choropleth map of Germany displaying average NO_2 concentrations in 2022, measured in micrograms per cubic meter (μg/m^3), across NUTS-3 regions. As presented on the map, western Germany has significantly higher NO_2 concentrations than eastern Germany. Notably, the highest concentrations are clustered in the Rhine–Ruhr metropolitan region in North Rhine–Westphalia, with additional hotspots along the Rhine corridor. In addition, Berlin appears as a distinct eastern hotspot. By contrast, the lowest NO_2 levels are concentrated in northeastern Germany, particularly in Mecklenburg-Vorpommern, Brandenburg (outside Berlin), Schleswig-Holstein, and large parts of Lower Saxony and Saxony-Anhalt. Central Germany also shows lower nitrogen dioxide levels.

Fig. 2b illustrates the trend in average NO_2 levels in Germany from 2018 to 2022. There has been a consistent decline in nitrogen dioxide levels, with a 27% decrease from 2018 to 2022. Among other drivers, this decline can be attributed to mobility and activity restrictions during the COVID-19 pandemic.

Spatial autocorrelation is the positive or negative correlation of a variable with itself due to the spatial location of the observations. Such spatial dependence can be due to the factors that are unobservable or difficult to quantify (Salima and Bellefon, 2018). The

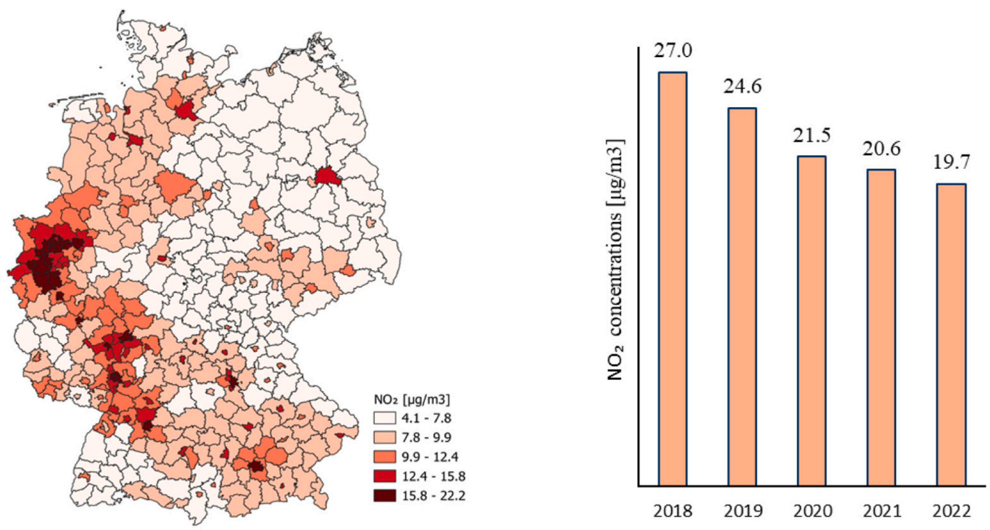

a) NUTS 3 level average NO_2 in Germany in 2022. *b) Country-level average NO_2 over 2018-2022.*

Fig. 2. NO_2 dispersion in Germany, a) per region on NUTS-3-level in 2022, b) as country-level average per year from 2018 to 2022. Source: Own illustration (European Environment Agency, 2022).

presence of spatial dependence in Germany can be statistically assessed using various techniques. Among the techniques, Moran's I, Geary's C, and spatial autoregression are the most widely applied (Shekhar and Xiong, 2007). In this study, Moran's I index is used, one of the earliest methods developed to measure spatial autocorrelation and still the standard tool today (Moran, 1950). A positive and significant Moran's I statistic indicates spatial clustering, whereas a negative and significant index indicates spatial dispersion. The null hypothesis for Moran's I index states that the values are randomly distributed across space; if the index is not significant, it provides no evidence against randomness. In this study, global Moran's I is applied to NO_2 data. In addition to the standard test, a permutation-based Moran's I is performed to protect against the errors that may result from the choice of spatial weights and from possible violations of the test's underlying assumptions (Bivand et al., 2013). In both the standard and permutation-based tests, Moran's I is positive and significant at the 1% level across all years. Positive and significant indices indicate that the null hypothesis that NO_2 is randomly distributed across Germany can be rejected. In other words, the statistics indicate that NO_2 concentrations tend to be spatially clustered in Germany. Global Moran's I tests and scatter plot analysis (see Fig. A.1 in the Appendix) confirm significant positive spatial autocorrelation, with NO_2 concentrations exhibiting clear high-high and low-low clustering across German NUTS-3 regions.

3. Methodology

3.1. Selection of variables

The research is conducted at the NUTS-3 regional level in Germany. Germany is divided into 400 NUTS-3 regions, corresponding to districts (Kreise) and independent cities (kreisfreie Städte) (Eurostat, 2025). Due to data limitations, seven regions are excluded from the analysis, resulting in a final sample of 393 regions. The study period spans the years 2018 to 2022. The dependent variable is the average concentration of nitrogen dioxide, measured in μg/m^3. The key explanatory variable in this study is clinker production. Because clinker production data are not available at the NUTS-3 level, clinker production is estimated from clinker plant CO_2 emissions using an emission intensity factor. Plant-level emissions data is provided by VDZ (Personal Communication), 2026. When selecting independent variables, it is important to isolate the effect of clinker production. Based on the literature review, this paper selects eight control variables. Three of these variables are GDP per capita (Li et al., 2020), population density (Zhao and Wang, 2022), and proportion of industrial value added (Li et al., 2018; Li et al., 2020; Thürkow et al., 2023). To test the Environmental Kuznets Curve (EKC) hypothesis in the German context, both GDP per capita and its squared terms are used. According to Thürkow et al. (2023), road transport is the largest contributor to nitrogen dioxide pollution in German urban areas. To account for this sector, two control variables are included. The first captures the vehicle fleet composition through the number of petrol and diesel passenger cars. The second variable is traffic-related accidents, serving as a proxy for traffic volume.

Li et al. (2020) include internal expenditure on scientific research funds as a control variable in their analysis of air pollution. Due to limited data availability, this study uses an alternative measure, the percentage of socially insured employees working in knowledge and research-intensive industries at the place of work. Thürkow et al. (2023) show that the combustion of coal, gas, solid biomass, and liquid fuels in private households is a significant source of nitrogen oxides in Germany. This implies that the household energy consumption structure is an important determinant of NO_2 pollution. However, data on the share of renewable energy use by households are not available at the county level. As a proxy, this study uses the share of newly completed residential buildings with renewable heating systems as the control variable. Meteorological conditions can also influence air pollution. Shen et al. (2021) show that higher NO_2 concentrations are generally associated with lower wind speeds. Because wind speed data are not available for NUTS-3 regions in Germany, this study follows the methodology of Angelova and Lupio (2020) to derive regional wind speed estimates from daily grid data (25 km × 25 km) provided by the Joint Research Center of European Commission (2025a). Wind speed is prioritized over other meteorological variables (e.g., temperature, precipitation, humidity) both because it is the most consistently identified driver of NO_2 dispersion in prior work (Shen et al., 2021) and because it is the only meteorological factor for which validated,

Table 1
Variable overview.

Variable	Definition	Unit	Data source
Poll	Average NO_2 concentrations	μg/m3	(European Environment Agency, 2025a)
Clinker	Amount of clinker production, derived from CO_2 emissions of clinker plants	ton	(VDZ, 2023) (CO_2 emission data)
Y	Per capita GDP (base period = 2010)	Euro	(Eurostat, 2026)
Pop	Population Density	Inhabitants per km^2	(BBSR, 2025)
Ind	Proportion of industrial value added in total value added.	%	
Car	Petrol and diesel passenger cars	per 1000 inhabitants	(Kraftfahrt Bundesamt, 2025)
Rd	Share of employees in knowledge and research-intensive industries (workplace-based)	%	(BBSR, 2025)
Wind	Average yearly wind speed	Meter per second	(Joint Research Center of European Commission, 2025b)
RenH	Percentage of completed residential buildings with renewable heating energy in newly constructed residential buildings	%	(BBSR, 2025)
Traf	Total road traffic accidents	per 100,000 inhabitants	(BBSR, 2025)

harmonized daily data at NUTS-3 resolution were available for the full 2018–2022 study period. The variable labels, definitions, units, and data sources for the regression models are presented in Table 1.

All variables in this study are log-transformed, except for those expressed as percentages to reduce estimation errors arising from heteroscedasticity and multicollinearity. Since the clinker production data is zero-inflated, the inverse hyperbolic sine (asinh) transformation is used in this study (see Eq. (1)). This transformation offers the advantages that it can be used without arbitrary manipulation of the original variable (Aihounton and Henningsen, 2021), while still allowing a similar interpretation of the coefficients to that of the log transformation (Bellemare and Wichman, 2020).

$$asinh(x) = ln\left(x + \sqrt{x^2 + 1}\right) \tag{1}$$

3.2. Model construction

The presence of spatial dependence in nitrogen dioxide requires spatial econometric models, as traditional regression approaches can yield biased and inconsistent estimates (Anselin, 1988). This arises because the assumption of independent samples in conventional econometric models is violated in the presence of spatial dependence (Zhao and Wang, 2022). Spatial econometric models effectively address the bias and inconsistency in coefficient estimates, thereby improving model accuracy and the reliability of statistical inference (Li et al., 2018).

The most used spatial econometric models in applied research are the Spatial Lag Model (SLM), the Spatial Error Model (SEM), and the SDM (Elhorst, 2010). The SDM has become particularly popular in the literature, and several studies have used it to disentangle direct and spillover effects on air pollution, including (Li et al., 2018; Feng et al., 2020; Li et al., 2020; Ding and Liu, 2023). Meanwhile, Zhao et al. (2020) used all three specifications (SLM, SEM, and SDM), while Ma et al. (2016) have employed the SLM framework in their studies. LeSage and Pace (2009) suggest that the selection of a spatial model should be made based on the likelihoods of different models. At the same time, the analysis should begin with a more general model to determine whether it should be reduced to SLM or SEM, based on the results of Wald and likelihood-ratio (LR) tests. In line with this approach, the present study also applies this ‘general to special’ framework. Additionally, a spatial Durbin error model (SDEM) is estimated to check for robustness. The SDM builds on the SLM by incorporating the spatial lag of the explanatory variables. This specification allows both the dependent variable and the regressors to generate spillover effects across regions, as shown in Eq. (2).

$$\begin{aligned} ln(Poll_{it}) = {} & a_0 + \rho W_i ln(Poll_t) + \beta_1 asinh(Clinker_{it}) + \beta_2 ln(Y_{it}) + \beta_3 ln(Y_{it})^2 + \beta_4 ln(Pop_{it}) + \beta_5 Ind_{it} + \beta_6 ln(Car_{it}) + \beta_7\, ln(Traf_{it}) \\ & + \beta_8 Rd_{it} + \beta_9 RenH_{it} + \beta_{10} ln(Wind_{it}) + W_i\, X_t \theta + u_{it} \end{aligned} \tag{2}$$

The SDEM does not include a spatially lagged dependent variable. Instead, it captures spatial dependence through spatially lagged explanatory variables and a spatially correlated error term, as specified in Eq. (3).

$$\begin{aligned} ln(Poll_{it}) = {} & a_0 + \beta_1 asinh(Clinker_{it}) + \beta_2 ln(Y_{it}) + \beta_3 ln(Y_{it})^2 + \beta_4 ln(Pop_{it}) + \beta_5 Ind_{it} + \beta_6 ln(Car_{it}) + \beta_7\, ln(Traf_{it}) + \beta_8 Rd_{it} + \beta_9 RenH_{it} \\ & + \beta_{10} ln(Wind_{it}) + W_i\, X_t \theta + u_{it}\; u_{it} = \lambda W_i u_t + \varepsilon_{it} \end{aligned} \tag{3}$$

Among them, i and t represent the county and year, respectively. W_i is the i_{th} row of the spatial matrix W, which is the $N \times N$ matrix with elements w_{ij}. $w_{ij} > 0$ if regions i and j are neighbors and $w_{ij} = 0$ otherwise; $w_{ii} = 0$ for all i. Variables indexed by t denote $N \times 1$ vector containing the respective values for all counties in year t. X_t is $N \times (K-1)$ matrix representing all control variables except for the squared GDP, and θ is the $(K-1) \times 1$ vector of coefficients, capturing spillover effects of the regressors. ρ is the spatial autoregressive coefficient, and λ is the spatial error coefficient.

While the ExternE Impact Pathway Approach relies on deterministic atmospheric dispersion modeling to link emissions to regional impacts (Bickel et al., 2005), the methodology of this study uses SDM to internalize these pathways statistically. The SDM's spatial weight matrix effectively serves as a proxy for the geographic and economic connectivity between regions. This allows to capture the net regional effect of clinker production, accounting for both the physical transport of pollutants and the secondary economic externalities, without the computational requirement of high-resolution meteorological simulations or specific logistics data.

A further advantage of the econometric framework adopted here is the ability to formally quantify estimation uncertainty through statistical inference. The direct and indirect effects are accompanied by standard errors derived from simulation-based impact decomposition, from which confidence intervals and significance levels are computed. Statistical significance at the 1% level indicates that the probability of observing an effect of this magnitude under the null hypothesis of no relationship is less than 1%, providing formal evidence that the estimated effects are distinguishable from random variation and model uncertainty. This is complementary to, but distinct from, cross-specification stability testing as part of sensitivity analyses. Together, within-specification inference and cross-specification robustness constitute the two standard criteria by which the reliability of econometric estimates can be assessed (LeSage and Pace, 2014).

3.3. Model selection

To decide whether SDM can be restricted to SLM or SEM, the likelihood ratio tests are used. Based on the test, the SDM model provides a significantly better fit than the SLM (LR $= 559.38$, $p < 0.001$), indicating that including spatially lagged explanatory variables substantially improves model performance. Similarly, the SDM significantly outperforms the SEM (LR = 46.77, $p < 0.001$), indicating that the spatial lag of explanatory variables accounts for more of the variation in the data than spatially correlated error terms alone. For reference, the SDM's own log-likelihood is 4178.01 (Table 2); the LR statistics above test this value against the nested SLM and SEM log-likelihoods. Model selection is corroborated beyond the LR tests by AIC, BIC, and R^2 comparisons across all five model classes (Table 2, Table A.6-Table A.12), which converge on the same preferred specification. Four SDM specifications are conducted to control for unobserved heterogeneity.

- No Fixed Effects (Pooled SDM): This is the baseline model without any fixed effects. It assumes that all spatial units and time periods share a common intercept.
- Time Fixed Effects: This specification controls unobserved shocks common to all districts in a given year (e.g., a pandemic) by including year-specific intercepts.
- Spatial Fixed Effects: This model includes spatial fixed effects (on a NUTS-2 level) to capture time-invariant unobserved characteristics of the region, such as geography.
- Two-Way Fixed Effects: This specification includes both time and spatial fixed effects to control both the region-specific and year-specific unobserved heterogeneity.

This paper uses a queen contiguity definition, where two regions are considered neighbors if they share (1) a common border or (2) a common vertex. Another commonly used spatial weight matrix is the inverse distance matrix, where the weight between two regions is calculated as the inverse of the distance between their centroids (1/d). The main reason for this choice is that several independent cities in Germany (*kreisfreie Städte*) are geographically located entirely within a surrounding district. In such cases, the centroid-to-centroid distance becomes extremely small, leading to disproportionately large weights in the inverse-distance calculation. For example, in the case of Spree-Neiße, the weight between Spree-Neiße and the kreisfreie Stadt Cottbus is 0.56, while the next-highest

Table 2
Direct, indirect, and total effects from SDM. Note: *, **, and *** indicate significance levels of 10%, 5%, and 1%, respectively.

	Baseline		Time FE		Spatial FE		Time & Spatial FE	
R-squared	0.791		0.854		0.887		0.906	
Adjusted R-squared	0.789		0.853		0.883		0.903	
Sigma^2	0.022		0.013		0.012		0.009	
Log-likelihood	4036.027		4070.746		4142.257		4178.012	
pho (ρ)	0.889	***	0.817	***	0.838	***	0.731	***
AIC	−8028.050		−8099.490		−8166.510		−8240.020	
BIC	−7905.220		−7982.240		−7837.100		−7916.190	
N	393		393		393		393	
Direct Effects								
asinh(Clinker)	0.004	**	0.004	***	0.005	***	0.005	***
ln(Y)	−1.396	***	−0.986	***	−0.663	**	−0.584	**
ln(Y)^2	0.068	***	0.049	***	0.033	**	0.030	**
ln(Pop)	0.191	***	0.193	***	0.193	***	0.191	***
Ind	0.001	***	0.001	**	0.002	***	0.001	**
ln(Car)	0.084	***	0.120	***	0.109	***	0.115	***
ln(Traf)	0.045	***	0.012		0.059	***	0.008	
Rd	−0.001	*	−0.002	***	−0.002	***	−0.002	***
RenH	−0.000	**	−0.000		−0.001	***	−0.000	*
ln(Wind)	−0.184	***	−0.160	***	−0.186	***	−0.160	***
Indirect (spillover) Effects								
asinh(Clinker)	0.034	**	0.023	**	0.032	**	0.021	***
ln(Y)	−9.575	**	−3.203	***	−0.967		−0.960	
ln(Y)^2	0.469	**	0.166	***	0.056		0.059	*
ln(Pop)	0.273	***	0.214	***	0.236	***	0.176	***
Ind	0.006	*	−0.000		0.007	*	−0.000	
ln(Car)	0.553	**	0.657	***	0.283		0.132	
ln(Traf)	0.351	***	−0.054		0.386	***	−0.095	
Rd	−0.006		−0.010	***	−0.013	**	−0.008	***
RenH	−0.006	***	−0.001		−0.010	***	−0.001	
ln(Wind)	−0.178		−0.164	*	0.371	**	0.113	
Total Effects								
asinh(Clinker)	0.038	**	0.024	**	0.036	**	0.026	***
ln(Y)	−10.971	**	−4.302	***	−1.630		−1.544	
ln(Y)^2	0.537	**	0.220	***	0.089		0.089	*
ln(Pop)	0.465	***	0.406	***	0.429	***	0.367	***
Ind	0.008	*	0.002		0.008	**	0.000	
ln(Car)	0.637	**	0.744	***	0.392		0.248	
ln(Traf)	0.396	***	−0.027		0.445	***	−0.087	
Rd	−0.007		−0.012		−0.015	***	−0.010	***
RenH	−0.006	***	−0.001	*	−0.011	***	−0.001	
ln(Wind)	−0.363	**	−0.332	***	0.185		−0.047	

weight, assigned to a bordering district, is only 0.048. This sharp contrast arises from the very short centroid-to-centroid distance between Cottbus and Spree-Neiße, because Cottbus is located within Spree-Neiße. However, air pollution easily disperses across borders, so such a large disparity in weights does not realistically capture the neighborhood structure relevant to pollution spillovers. Indeed, another paper studying spatial spillover effects of environmental pollution in Germany uses a queen-based spatial weight matrix (Rüttenauer, 2018). However, as a common practice, the model is also estimated using an inverse distance weight matrix, with the corresponding results presented in the robustness check section.

4. Results

4.1. Main model

Table 2 reports the estimated direct, indirect, and total impacts of the models, along with key model diagnostics and spatial correlation parameter (ρ). The corresponding coefficient estimates from the regression summaries are reported in the Appendix (see Table A.1, Table A.2, Table A.3, and Table A.4).

Based on model diagnostics, the specification with both time and spatial fixed effects is preferred, as it has the highest explanatory power (R-squared and log-likelihood) and the lowest AIC and residual variance. Therefore, this model is the primary focus for interpretation, with other specifications referenced occasionally for comparison.

Across all the SDM specifications, direct and indirect effects of clinker production on NO_2 pollution are significant. That means clinker production not only affects pollution locally but also causes pollution to cross regional boundaries. More precisely, a 1 % increase in clinker production within a given NUTS-3 region raises local NO_2 levels by 0.005%, reflecting the direct effect of clinker production. The spillover effects of clinker production are even stronger: a comparable increase in clinker production in neighboring regions raises NO_2 levels in the region by 0.021%. The indirect effect is estimated at 0.02120 (standard error = 0.00680, 95% confidence interval [0.008, 0.035]). Since the indirect spillover effect (0.02120) is more than three times larger than the standard error (0.00680), the standard uncertainty measure, and the confidence interval is entirely above zero. As a result, the spillover effect can be distinguished from random noise, as even considering the full range of model uncertainty, the effect remains positive and significant (compare Table A.15). This result is consistent with Li et al. (2020), who report that cement production generates stronger spillover effects than direct effects.

In all specifications, both GDP in logarithmic form and its squared term are statistically significant, with coefficients of −0.584 and 0.030, respectively. The combination of a negative and significant coefficient on the linear GDP term with a positive and significant coefficient on its squared term is the standard signature of a U-shaped (as opposed to inverted-U, EKC-consistent) relationship in this literature. This indicates that the relationship between economic output and air pollution across German districts follows a U-shaped pattern, which contrasts with Kuznets's inverted-U-shape hypothesis. The result is similar to the findings of Destek et al. (2018), who report a U-shaped relationship between air pollution and economic growth in EU countries. In addition, another study examining the EKC hypothesis across 401 districts in Germany, using nitrogen surplus as an environmental pollutant and median monthly wage as an economic growth indicator, finds no inverted-U-shaped relationship (Castro Campos and Petrick, 2023). This study's findings indicate that pollution does not decline continuously as GDP rises in Germany. Within a given county, as GDP per capita rises over the study period, pollution first tends to fall. Still, beyond a threshold, further increases in GDP per capita are associated with higher pollution levels.

Both the direct and indirect effects of population density on air pollution are positive and significant across all specifications. A 1% increase in the number of people per square kilometer in a district raises NO_2 concentrations in that district by about 0.19%. In comparison, a 1 % increase in population density in neighboring districts increases local NO_2 concentrations by approximately 0.18%. There is a variety of literature studying the relationship between population density and air pollution, and the results consistently show that higher population density is associated with higher levels of environmental pollutants (Borck and Schrauth, 2021; Wrightson et al., 2025).

Another significant factor in NO_2 pollution is the industrial structure of regions. Across all model specifications, the direct impact of industrial activity on NO_2 concentrations is positive and statistically significant, with estimated coefficients ranging from 0.001 to 0.002. That means a 1 %age point increase in the proportion of industrial value-added increases air pollution by 0.1%. These findings align with those of Li et al. (2018), who document that industrial activities increase air pollution. Another measure of the economy's structure, the share of the tertiary (service) sector, is also tested. The coefficient is negative and statistically significant (−0.001), indicating that a higher share of the service sector, relative to industrial activity, reduces pollution.

As expected, diesel and petrol cars increase air pollution in the regions. An increase of one percent in the number of petrol and diesel cars per 1000 inhabitants raises NO_2 concentrations in the same district by about 0.12%. The role of diesel cars in creating NO_2 concentrations is widely discussed in the literature. Evidence from Norway shows that among passenger cars, diesel cars account for the largest share of total road traffic NO_X emissions (47.9%), followed by petrol cars (4.9%). At the same time, other vehicle types contribute only marginally (Wærsted et al., 2022). Given this substantial difference in emission profiles, the model is re-estimated to include only diesel cars instead of both petrol and diesel cars. A higher coefficient is expected, given that diesel cars pollute far more than petrol cars. However, the estimated effect remained similar (0.11). This result can be explained by the high correlation between diesel and petrol car ownership (0.95), meaning that regions with more diesel cars also tend to have more petrol cars, and vice versa. Another transportation-related variable, traffic accidents, shows positive direct and spillover effects in two specifications but loses significance in the main specification. This may indicate that traffic accident data do not adequately capture traffic volume. Perhaps with more direct measures of traffic, such as traffic counts or road-congestion data, the result could be more robust.

According to the estimates, a higher share of employees in knowledge- and research-intensive industries is associated with lower levels of air pollution, as reflected by negative direct (−0.002) and indirect (−0.008) effects. This finding is expected, as regions with a stronger concentration of R&D-intensive sectors tend to adopt cleaner technologies. Another variable expected to reduce pollution in the NUTS-3 regions is the share of newly constructed residential buildings equipped with renewable heating systems. In the main model, the spillover effects of this variable are not significant, whereas its direct impact is significant at the 10% level.

The direct impact of wind speed on air pollution is robust across all model specifications. As expected, higher wind speeds reduce pollutant concentrations within a region. A 1% increase in wind speed lowers NO_2 concentrations by about 0.16%. However, no significant spillover effects are observed.

The spatial autoregressive coefficient, rho, is significant and estimated at 0.73, indicating spatial correlation of NO_2 concentrations across NUTS-3 districts. This implies that air pollution levels in one district are strongly influenced by those in neighboring districts, as indicated by Moran's I.

4.2. Robustness and model sensitivity

To verify the stability of the baseline results, a series of robustness checks across three dimensions is performed: spatial weighting, econometric specification, and sample restriction. First, the SDM is re-estimated using an inverse-distance spatial weights matrix to account for a broader definition of regional connectivity. As shown in Table A.5 and Table A.7, the clinker effect remains positive and significant. While the magnitude of spillovers increases under distance-based weights (0.09% vs. 0.021%), the baseline queen-contiguity specification remains the superior model based on AIC, BIC, and log-likelihood diagnostics. Second, alternative econometric specifications are tested, including the SDEM, spatial autoregressive model (SAR), and SEM (Table A.6 through Table A.12). Across all specifications, clinker production consistently exerts both direct and indirect upward pressure on NO_2 concentrations. The SDM, however, consistently provides the best fit (R2 = 0.906), justifying its use as the primary model.

Finally, the study addressed potential spatial decay by restricting the analysis to a 60 km buffer zone around clinker-producing plants, following the effective spillover distances identified in previous literature (Wang et al., 2017). Results from this restricted sample (Table A.13, Fig. A.2) align closely with the national baseline, with the indirect effect remaining identical (0.021%) and the direct effect slightly increasing (0.006%). Throughout these tests, the direction and significance of all control variables, including the U-shaped GDP-pollution relationship, urban density, and vehicle fleet composition, remained remarkably stable, confirming the reliability of the main empirical findings.

Taken together, these checks address concerns about model uncertainty directly: rather than relying on a single specification, the clinker effect is re-estimated under five model classes (SDM, SLM, SEM, SDEM, SAR), two spatial weighting schemes, and two sample definitions. The coefficient remains positive and statistically significant (at minimum at 5% level) in every case, with point estimates

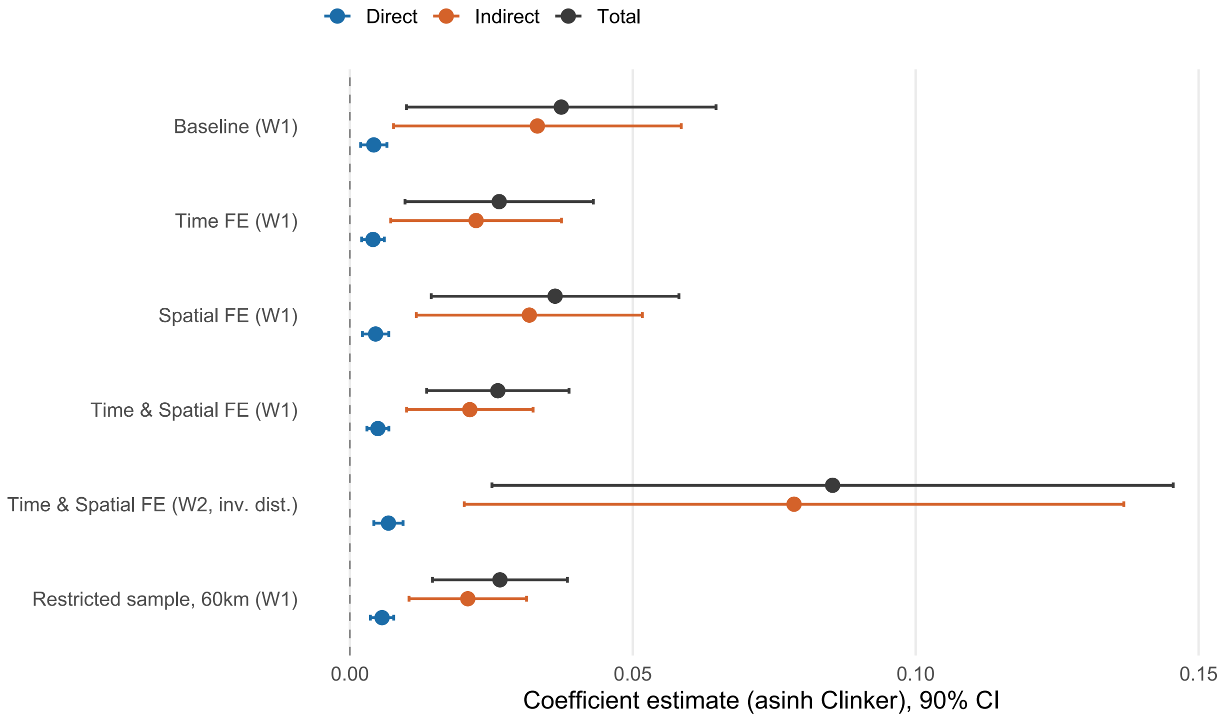

Fig. 3. Stability of the clinker effect on NO_2 across specifications, main models (W1) plus inverse-distance weights and 60 km buffer robustness checks. Source: Own calculations.

for the indirect effect ranging narrowly between 0.018 and 0.09 across specifications. This consistency in sign, significance, and order of magnitude across structurally different model assumptions is the standard criterion in the spatial econometrics literature for distinguishing genuine effects from artifacts of a single model specification (LeSage and Pace, 2009). Fig. 3 visualizes this stability across the four primary SDM specifications. The wider confidence interval associated with the inverse-distance weight matrix (W2) reflects the greater spatial reach of this weighting scheme, which amplifies the variance of estimated spillover effects relative to the more conservative queen-contiguity specification (W1), while the point estimate remains positive and statistically significant.

The small absolute magnitude of the coefficients reflects the scale of clinker production relative to total regional NO_2 concentrations and should not be interpreted as evidence of unreliability; rather, it is consistent with the expectation that a single industrial source category contributes a modest but measurable share of overall pollution at the district level.

4.3. Discussion

Externalities, defined as the unintended costs or benefits of an activity borne by third parties, are a central source of market failure. While initial studies emphasized the economic and social dimensions of externalities, the focus has gradually shifted toward environmental externalities (Radukić and Perović, 2019). In this paper, the regional externalities of clinker production are examined by analyzing its spatial spillover effects on air pollution across the NUTS-3 region. The results confirm the existence of environmental externalities: clinker plants not only pollute their host regions but also affect neighboring districts. In fact, the finding that spillover impacts (0.021%) exceed direct effects (0.005%) aligns with spatial econometric theory regarding the transboundary nature of atmospheric pollutants (Anselin, 2001; Sun et al., 2024). These findings suggest that effective mitigation policies for air pollution require coordinated, joint governance, as air pollution is not confined to local boundaries. Another interesting finding is the U-shaped relationship between economic growth, measured by GDP per capita, and air pollution, measured by average NO_2 concentrations. Halkos (2011) identifies an N-shaped relationship between economic growth and pollution for 32 countries, including Germany. While a U-shaped result may seem to diverge from standard EKC expectations, it likely represents a localized scale effect or a rebound effect within the broader N-shaped trajectory (Dinda, 2004). It is possible that Germany is currently situated in the U-shaped segment of this broader N-shaped trajectory, where recent industrial intensity temporarily outpaces technical efficiency gains (Alvarez-Herranz et al., 2017).

Furthermore, beyond replicating the transboundary patterns identified by physical dispersion models, the statistical approach adopted here offers two distinct advantages. First, it does not require high-resolution meteorological or stack-level emissions data, which are often unavailable at fine spatial granularity, making the method readily applicable to other regions or pollutants with comparable data constraints. Second, and more importantly, it captures channels of spatial dependence that dispersion models are not designed to detect, such as the clustering of supply chains, heavy-duty logistics, and shared industrial infrastructure around clinker production hubs. These economic co-effects can themselves generate or amplify pollution in neighboring regions independent of atmospheric transport, meaning the spillover estimated here likely reflects a broader regional externality than physical dispersion alone. This complements rather than substitutes for dispersion modeling, which remains better suited to fine-grained, mechanistic attribution of pollutant transport (Thunis et al., 2019).

However, further research is required to confirm this dynamic. The analysis focuses on socioeconomic and meteorological determinants of regional NO_2 concentrations and does not account for all potential emission sources. In the German context, this is unlikely to substantially affect the results, e.g., seaport activity is confined to a small number of coastal districts, and road transport, which is the dominant source of NO_2 in German regions, is explicitly controlled for. Stationary combustion sources such as thermal power plants remain a relevant avenue for future work. Plant-level emission inventories such as the *E*-PRTR could complement this framework, though their coverage is limited to facilities above reporting thresholds (OECD, 2025).

The findings of this study show that population density significantly affects air pollution, underscoring the role of urban planning. In addition, the paper shows how vehicle fleet composition is important for air pollution. Transitioning from diesel and petrol vehicles to low-emission alternatives can reduce pollution. Beyond the factors that worsen air quality, the analysis shows that a higher share of employment in knowledge and research-intensive industries is associated with lower pollution levels. Similarly, the share of renewable heating systems in newly constructed houses is significantly associated with lower air pollution, although only at the 10% significance level. This underscores the potential for technological decoupling in the residential sector, as noted in EU industrial benchmarks (Schorcht et al., 2013). Incorporating a more direct measure of regional investment in R&D and household use of renewable energy could strengthen the results. Lastly, the analysis indicates that meteorological conditions also influence air quality. In particular, wind contributes to pollutant dispersion, reducing air pollution in the region. This underlines the importance of accounting for meteorological factors when analyzing air pollution dynamics.

However, the results are subject to limitations inherent in statistical modeling. Like all source apportionment methods, the estimated effects of clinker production on regional NO_2 are influenced by uncertainties in data quality, satellite pollution measurements, emission proxies, and the spatial weight matrix. Sensitivity analyses in Section 4.2 show the effects' significance and magnitude are stable across eleven models. However, the absolute coefficients should be interpreted cautiously, as the main contribution is identifying a consistent, significant transboundary externality, not precise estimates.

5. Conclusion

Germany's emissions from clinker production are a significant share of overall industrial emissions, underscoring the need for mitigation in this sector. Hence, this paper develops spatial econometric models to quantify the impact of clinker production on NO_2

emissions, accounting for both local effects and spill over in neighboring areas. Using panel data covering 393 counties for the period 2018–2022, the analysis employs the SDM as the main specification. The results show that clinker production significantly contributes to air pollution. Specifically, a 1% increase in clinker production within a region raises its local NO_2 concentration by 0.005%. A similar increase in clinker production in neighboring regions leads to a 0.021% rise in local NO_2 levels, indicating that spillover effects are greater than direct effects. The results provide clear evidence of regional environmental externalities, meaning that pollution generated in one area affects air quality in surrounding regions. This suggests that effective NO_2 mitigation in Germany requires coordinated regulation and joint governance across neighboring regions. By establishing that spillover effects are a dominant driver of local pollution levels, this study reinforces the necessity of moving beyond localized emission targets toward a spatially integrated policy framework. Such a framework accounts for the 'spatial lag' inherent in industrial emissions, ensuring that mitigation efforts in one district are not undermined by industrial intensification in another. In addition, recognizing these externalities is essential to market efficiency. Hence, further research quantifying these regional externalities would be important. Such evidence would enable policymakers to develop instruments that effectively internalize these spillovers, for example, through cost-sharing or compensation mechanisms between clinker-producing regions and those affected by their pollution.

CRediT authorship contribution statement

N. Ahmadova: Writing – Original Draft, Writing – Review & Editing, Validation, Investigation, Conceptualization, Formal analysis, Data curation, Methodology, Software, Visualization. I. Rhoden: Conceptualization, Writing – Review & Editing, Validation, Funding Acquisition, Supervision. S. Vögele: Writing – Review & Editing, Supervision. J. Linßen: Funding Acquisition, Supervision.

Funding

This work was supported by the Helmholtz Association, Germany, under the Innovation Pool Project "Industrial Transformation 2050" (IT2025) and under the program "Energy System Design".

Declaration of competing interest

The authors declare that they have no known competing financial interests or personal relationships that could have appeared to influence the work reported in this paper.

Acknowledgements

The authors gratefully thank Debapratim Mukherjee for his valuable support in the data collection process. During the preparation of this work, the authors used DeepL in order to improve readability and the language. After using this tool, the authors reviewed and edited the content as needed and take full responsibility for the content of the publication.

Appendix A

Spatial autocorrelation

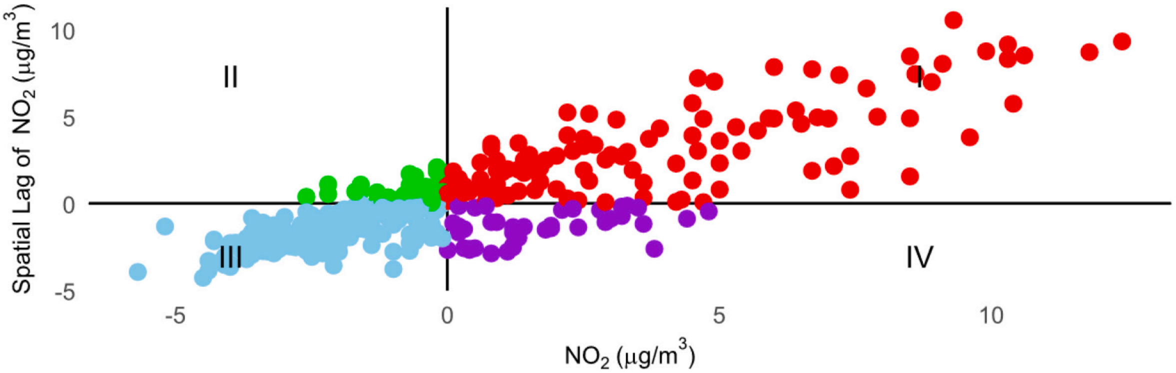

Fig. A.1. Moran scatter plot of NO_2 in Germany, 2022. Source: Own calculation.

Full SDM coefficients corresponding to Table 2

Table A.1
SDM without fixed effects.

Variable	Estimate		Std. Error	t value	Pr(>|t|)
(Intercept)	5.683	**	2.541	2.237	0.0254
asinhclinker	0.003	***	0.001	2.764	0.0058
Ind	0.001	***	0.000	3.988	0.0001
lnY	−0.920	***	0.231	−3.979	0.0001
lnY^2	0.045	***	0.011	4.083	0.0000
lnPop	0.178	***	0.004	45.814	0.0000
lnCar	0.058	**	0.024	2.389	0.0170
lnTraf	0.028	**	0.012	2.375	0.0176
Rd	−0.001	*	0.000	−1.803	0.0716
RenH	−0.000		0.000	−0.430	0.6674
lnWind	−0.176	***	0.022	−8.158	0.0000
Wlag.asinhclinker	0.002		0.002	1.100	0.2717
Wlag.Ind	−0.000		0.000	−0.391	0.6958
Wlag.lnY	−0.333		0.439	−0.758	0.4485
Wlag.lnY^2	0.017		0.021	0.785	0.4326
Wlag.lnPop	−0.125		0.005	−26.331	0.0000
Wlag.lnCar	0.016		0.036	0.434	0.6645
Wlag.lnTraf	0.018		0.018	1.008	0.3138
Wlag.Rd	−0.000		0.001	−0.116	0.9076
Wlag.RenH	−0.001	***	0.000	−2.671	0.0076
Wlag.lnWind	0.136	***	0.029	4.679	0.0000
rho	0.889	***	0.009	94.193	0.0000

Table A.2
SDM with time fixed effects.

Variable	Estimate		Std. Error	t value	Pr(>|t|)
asinhclinker	0.003	***	0.001	2.942	0.0033
lnY	−0.781	***	0.233	−3.348	0.0008
lnY^2	0.038	***	0.011	3.466	0.0005
lnPop	0.179	***	0.004	45.856	0.0000
Ind	0.001	***	0.000	3.302	0.0010
lnCar	0.077	***	0.024	3.172	0.0015
lnTraf	0.016		0.012	1.347	0.1780
Rd	−0.001	***	0.000	−2.595	0.0095
RenH	−0.000		0.000	−1.158	0.2470
lnWind	−0.150	***	0.020	−7.579	0.0000
Wlag.asinhclinker	0.002		0.002	1.223	0.2217
Wlag.lnY	0.015		0.051	0.286	0.7749
Wlag.lnY^2	0.001		0.003	0.403	0.6870
Wlag.lnPop	−0.105	***	0.005	−21.933	0.0000
Wlag.Ind	−0.001	*	0.000	−1.811	0.0703
Wlag.lnCar	0.064	*	0.036	1.790	0.0735
Wlag.lnTraf	−0.024		0.016	−1.478	0.1396
Wlag.Rd	−0.001	*	0.001	−1.784	0.0746
Wlag.RenH	−0.000		0.000	−0.484	0.6284
Wlag.lnWind	0.091		0.026	3.446	0.0006
rho	0.817		0.014	60.434	0.0000

Table A.3
: SDM with spatial fixed effects.

Variable	Estimate		Std. Error	t value	Pr(>|t|)
(Intercept)	0.310		3.368	0.092	0.927
asinhclinker	0.003	***	0.001	2.951	0.003
lnY	−0.600	**	0.247	−2.431	0.015
lnY^2	0.030	**	0.012	2.542	0.011
lnPop	0.180	***	0.004	44.883	0.000
Ind	0.001	***	0.000	4.530	0.000
lnCar	0.093	***	0.026	3.520	0.000
lnTraf	0.037	***	0.012	3.110	0.002
Rd	−0.001	***	0.000	−3.364	0.001
RenH	−0.000	*	0.000	−1.897	0.058

(*continued on next page*)

Table A.3 (*continued*)

Variable	Estimate		Std. Error	t value	Pr(>|t|)
lnWind	−0.207	***	0.022	−9.484	0.000
Wlag.asinhclinker	0.003	*	0.002	1.820	0.069
Wlag.lnY	0.363		0.545	0.667	0.505
Wlag.lnY^2	−0.017		0.026	−0.634	0.526
Wlag.lnPop	−0.111	***	0.008	−14.234	0.000
Wlag.Ind	0.000		0.001	0.046	0.963
Wlag.lnCar	−0.032		0.061	−0.526	0.599
Wlag.lnTraf	0.034	*	0.019	1.781	0.075
Wlag.Rd	−0.001		0.001	−1.242	0.214
Wlag.RenH	−0.001	***	0.000	−5.510	0.000
Wlag.lnWind	0.237	***	0.033	7.209	0.000
rho	0.838	***	0.013	66.656	0.000

Table A.4
SDM with time and spatial fixed effects.

Variable	Estimate		Std. Error	t value	Pr(>|t|)
asinhclinker	0.003	***	0.001	3.70	0.000
lnY	−0.512	**	0.247	−2.08	0.038
lnY^2	0.026	**	0.012	2.23	0.026
lnPop	0.179	***	0.004	44.48	0.000
Ind	0.001	***	0.000	3.05	0.002
lnCar	0.106	***	0.027	3.94	0.000
lnTraf	0.015		0.013	1.22	0.221
Rd	−0.001	***	0.000	−3.32	0.001
RenH	−0.0002	*	0.000	−1.84	0.065
lnWind	−0.168	***	0.020	−8.25	0.000
Wlag.asinhclinker	0.003	**	0.002	1.998	0.046
Wlag.lnY	0.099		0.087	1.141	0.254
Wlag.lnY^2	−0.002		0.004	−0.511	0.610
Wlag.lnPop	−0.080	***	0.008	−10.231	0.000
Wlag.Ind	−0.001		0.000	−1.515	0.130
Wlag.lnCar	−0.038		0.060	−0.626	0.531
Wlag.lnTraf	−0.038	**	0.018	−2.044	0.041
Wlag.Rd	−0.001		0.001	−1.466	0.143
Wlag.Ren	0.000		0.000	0.172	0.864
Wlag.lnWind	0.155	***	0.030	5.231	0.000
rho	0.731	***	0.019	39.108	0.000

Alternative spatial weight matrices

Table A.5
SDM estimates with inverse distance spatial weight matrix. Note: *, **, and *** indicate significance levels of 10%, 5%, and 1%, respectively. X and W*X columns present coefficients for explanatory variables and their spatial lags, respectively. DE, IE and TE stand for direct effect, indirect effect and total effect, respectively. Both time and spatial fixed effects are included.

	X		W*X		DE		IE		TE	
asinh(Clinker)	0.005	***	0.016	*	0.007	***	0.086	**	0.093	***
lnY	−1.237	***	0.524	***	−1.302	***	−1.618		−2.920	**
lnY^2	0.061	***	−0.024	***	0.064	***	0.089		0.153	**
lnPop	0.198	***	−0.054	***	0.207	***	0.359	***	0.566	***
Ind	0.001	***	0.0004		0.001	***	0.006		0.007	
lnCar	0.135	***	−0.352	***	0.121	***	−1.089	**	−0.968	*
lnTraf	−0.008		−0.062	**	−0.015		−0.311	**	−0.326	**
Rd	−0.002	***	−0.005	***	−0.002	***	−0.024	***	−0.027	***
Ren	−0.001	***	−0.000		−0.001	***	−0.004	**	−0.005	***
lnWind	−0.114	***	0.096	**	−0.119	***	0.059		−0.061	
ρ	0.751	***								
R-squared	0.906									
Adj. R-squared	0.903									
Sigma^2	0.009									
Log-likelihood	3906.421									
AIC	−7705.41									
BIC	−7381.59									
N	393									

Alternative model specifications

Table A.6
SDEM estimates with two spatial weight matrices Note: *, **, and *** indicate significance levels of 10%, 5%, and 1%, respectively. X and W*X columns present coefficients for explanatory variables and their spatial lags, respectively.

	Under W1 (queen based)				Under W2 (inverse distance-based)			
	X		W*X		X		W*X	
asinh(Clinker)	0.004	***	0.009	***	0.006	***	0.026	***
lnY	−0.482	**	−0.454	***	−1.111	***	−0.210	
lnY^2	0.025	**	0.026	***	0.054	***	0.007	
lnPop	0.193	***	0.086	***	0.208	***	0.146	***
Ind	0.001	***	0.0003		0.001	***	0.002	
lnCar	0.178	***	0.298	***	0.201	***	0.278	*
lnTraf	0.014		−0.069	**	−0.017		−0.181	***
Rd	−0.002	***	−0.002	*	−0.002	***	−0.008	***
RenH	−0.0004	**	−0.001	***	−0.001	***	−0.004	***
lnWind	−0.217	***	0.058		−0.151	***	0.082	
lambda (λ)	0.833	***			0.826	***		
R-squared	0.864				0.887			
Adj. R-squared	0.860				0.883			
Sigma2	0.013				0.010			
Log-likelihood	4145.039				3856.696			
AIC	−8174.08				−7597.39			
BIC	−7850.25				−7273.56			
N	393				393			

Table A.7
SDM estimates with inverse distance spatial weight matrix. Note: *, **, and *** indicate significance levels of 10%, 5%, and 1%, respectively. X and W*X present coefficients for clinker production and its spatial lag, respectively.

	SAR		SEM		SDM		SDEM	
X	0.004	***	0.002	**	0.003	***	0.004	***
W*X					0.003	***	0.009	***
DE	0.005	***			0.005	***		
IE	0.004	***			0.021	***		
TE	0.009	***			0.026	***		
rho(ρ)	0.516	***			0.731	***		
lambda (λ)			0.907	***			0.833	***
R-squared	0.893		0.767		0.906		0.864	
Adj. R-squared	0.891		0.761		0.903		0.860	
Sigma2	0.01		0.022		0.009		0.013	
Log-likelihood	4030.368		4023.052		4178.012		4145.039	
AIC	−7964.74		−7950.1		−8240.02		−8174.08	
BIC	7696.74		−7682.11		−7916.19		−7850.25	
N	393		393		393		393	

Table A.8
Model results for clinker production under W2. Note: *, **, and *** indicate significance levels of 10%, 5%, and 1%, respectively. X and W*X present coefficients for clinker production and its spatial lag, respectively.

	SAR		SEM		SDM		SDEM	
X	0.006	***	0.005	**	0.005	***	0.006	***
W*X					0.016	***	0.026	***
DE	0.006	***			0.007	***		
IE	0.023	***			0.086	***		
TE	0.029	***			0.093	***		
rho(ρ)	0.789	***			0.751	***		
lambda (λ)			0.907	***			0.826	***
R-squared	0.827		0.891		0.906		0.887	

(*continued on next page*)

Table A.8 (*continued*)

	SAR	SEM	SDM	SDEM
Adj. R-squared	0.823	0.889	0.903	0.883
Sigma squared	0.02	0.01	0.009	0.010
Log-likelihood	3711.219	3629.361	3906.421	3856.696
AIC	−7326.44	−7162.72	−7705.41	−7597.39
BIC	−7058.44	−6894.73	−7381.59	−7273.56
N	393	393	393	393

Table A.9
SAR model with time and spatial fixed effects under W1.

Variable	Estimate		Std. Error	t value	Pr(>|t|)
asinhclinker	0.004	***	0.001	4.111	0.000
lnY	−0.186		0.265	−0.703	0.482
lnY^2	0.011		0.013	0.908	0.364
lnPop	0.171	***	0.004	44.574	0.000
Ind	0.000		0.000	1.591	0.112
lnCar	0.095	***	0.029	3.243	0.001
lnTraf	0.011		0.014	0.827	0.408
Rd	−0.002	***	0.000	−3.194	0.001
RenH	−0.000	**	0.000	−2.338	0.020
lnWind	−0.079	***	0.016	−4.840	0.000
rho	0.516	***	0.015	35.460	0.000

Table A.10
SAR model with time and spatial fixed effects under W2.

Variable	Estimate		Std. Error	t value	Pr(>|t|)
asinhclinker	0.006	***	0.001	4.8735	0.000
lnY	−1.445	***	0.319	−4.5298	0.000
lnY^2	0.070	***	0.015	4.6022	0.000
lnPop	0.211	***	0.005	45.737	0.000
Ind	0.001	***	0.000	3.9826	0.000
lnCar	0.216	***	0.035	6.1616	0.000
lnTraf	−0.005		0.016	−0.2793	0.780
Rd	−0.002	***	0.001	−4.2802	0.000
RenH	−0.001	***	0.000	−4.7704	0.000
lnWind	−0.038	*	0.020	−1.9344	0.053
rho	0.789	***	0.03	26.0280	0.000

Table A.11
SEM with time and spatial fixed effects under W1.

Variable	Estimate		Std. Error	t value	Pr(>|t|)
asinhclinker	0.002	**	0.001	2.475	0.013
lnY	−1.210	***	0.215	−5.618	0.000
lnY^2	0.057	***	0.010	5.636	0.000
lnPop	0.185	***	0.004	46.853	0.000
Ind	0.001	***	0.000	5.821	0.000
lnCar	0.121	***	0.025	4.845	0.000
lnTraf	0.031	**	0.012	2.521	0.012
Rd	−0.001	***	0.000	−3.310	0.001
RenH	−0.0001		0.000	−0.875	0.382
lnWind	−0.190	***	0.021	−8.855	0.000
lambda	0.907	***	0.012	76.369	0.000

Table A.12
SEM with time and spatial fixed effects under W2.

Variable	Estimate		Std. Error	t value	Pr(>|t|)
asinhclinker	0.005	***	0.001	4.163	0.000
lnY	−1.565	***	0.329	−4.751	0.000
lnY^2	0.074	***	0.016	4.758	0.000
lnPop	0.220	***	0.005	45.477	0.000
Ind	0.002	***	0.000	5.428	0.000
lnCar	0.245	***	0.036	6.763	0.000
lnTraf	−0.017		0.017	−0.992	0.321
Rd	−0.003	***	0.001	−4.958	0.000
RenH	−0.001	***	0.000	−4.433	0.000
lnWind	−0.036	*	0.021	−1.719	0.086
lambda	0.895	***	0.017	57.885	0.000

Restricted spatial sample

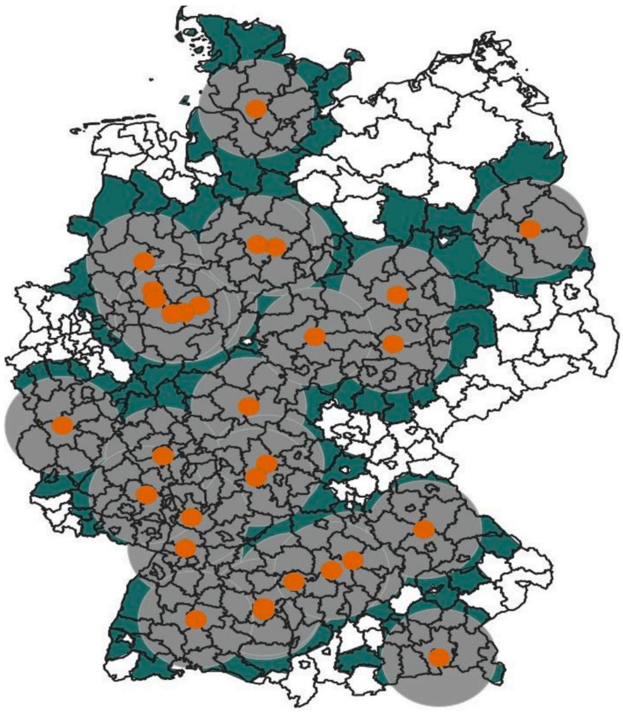

Fig. A.2. Clinker Plants with buffer zones (60 km radius). Clinker plants are shown by orange points, and their 60 km buffer zones are depicted by grey circles. NUTS-3 regions intersecting with at least one buffer zone are highlighted in dark red, the number of NUTS-3 regions in the buffered zones is 293. Source: Own illustration (Eurostat, 2025; VDZ, 2025). (For interpretation of the references to colour in this figure legend, the reader is referred to the web version of this article.)

Table A.13
SDM estimation results for the restricted sample. Note: *, **, and *** indicate significance levels of 10%, 5%, and 1%, respectively.

	Under W1 (queen based)						Under W2 (inverse distance-based)					
	DE		IE		TE		DE		IE		TE	
asinh (Clinker)	0.006	***	0.021	***	0.027	***	0.008	***	0.074	**	0.081	**
lnY	−0.780	**	−0.851		−1.623	*	−1.004	***	0.632		−0.373	
lnY^2	0.040	**	0.051		0.089	*	0.050	***	0.007		0.056	
lnPop	0.211	***	0.167	***	0.377	***	0.225	***	0.178	**	0.403	***
Ind	0.002	***	0.003		0.005	*	0.003	***	0.015	**	0.017	***
lnCar	0.207	***	0.017		0.223		0.203	***	−1.808	***	−1.606	***
lnTraf	0.010		−0.108		−0.102		−0.018		−0.493	***	−0.511	***
Rd	−0.003	***	−0.009	**	−0.012	***	−0.004	***	−0.029	***	−0.033	***
RenH	−0.001	***	−0.002	**	−0.003	***	−0.002	***	−0.006	***	−0.007	***
lnWind	−0.092	***	0.185	**	0.101		−0.075	***	0.362	**	0.287	***
ρ					0.689	***	0.693	***				
R-squared	0.890						0.890					
Adj. Rsquared	0.886						0.886					
Sigma squared	0.009						0.009					
Log-likelihood	3047.443						2890.256					
AIC	−5990.89						−5676.51					
BIC	−5716.54						−5402.17					
N	293						293					

Table A.14
SDM estimations for the restricted sample.

	Under W1 (queen based)				Under W2 (inverse-distance based)			
	X		W*X		X		W*X	
asinh(Clinker)	0.004	***	0.004	**	0.006	***	0.018	**
lnY	−0.735	**	0.234	**	−1.013	***	0.906	***

(continued on next page)

Table A.14 (*continued*)

	Under W1 (queen based)				Under W2 (inverse-distance based)			
	X		W*X		X		W*X	
lnY^2	0.036	***	−0.008		0.049	***	−0.032	***
lnPop	0.199	***	−0.082	***	0.221	***	−0.099	***
Ind	0.002	***	−0.001		0.002	***	0.003	
lnCar	0.206	***	−0.139	*	0.251	***	−0.731	***
lnTraf	0.016		−0.048	**	−0.006		−0.147	***
Rd	−0.002	***	−0.001		−0.003	***	−0.007	***
RenH	−0.001	***	−0.0002		−0.002	***	−0.001	
lnWind	−0.106	***	0.135	***	−0.083	***	0.171	***

Table A.15
Impact decomposition for variable asinhClinker, from the main model (preferred specification SDM, two-way fixed effects), with standard errors and 95% confidence intervals.

Effect	Estimate	Std. Error	95% CI
Direct	0.005	0.001	[0.003, 0.007]
Indirect	0.021	0.007	[0.008, 0.035]
Total	0.026	0.008	[0.011, 0.041]

Data availability

Data will be made available on request.

References

Aihounton, G.B., Henningsen, A., 2021. Units of measurement and the inverse hyperbolic sine transformation. Econ. J. 24 (2), 334–351. https://doi.org/10.1093/ectj/utaa032.

Alvarez-Herranz, A., Balsalobre-Lorente, D., Shahbaz, M., Cantos, J.M., 2017. Energy innovations-GHG emissions Nexus: fresh empirical evidence from OECD countries. Energy Policy 101, 90–100. https://doi.org/10.1016/j.enpol.2016.11.030.

Angelova, D., Lupio, N.B., 2020. Constructing a meteorological indicator dataset for selected European NUTS 3 regions. Data Brief 31, 105786. https://doi.org/10.1016/j.dib.2020.105786.

Anselin, L., 1988. Spatial Econometrics: Methods and Models. Springer Science & Business Media.

Anselin, L., 2001. Spatial econometrics. In: A Companion to Theoretical Econometrics, pp. 310–330. https://doi.org/10.1002/9780470996249.ch15.

BBSR, 2025. INKAR-Indikatoren und Karten zur Raum- und Stadtentwicklung. https://www.inkar.de.

Bellemare, M.F., Wichman, C.J., 2020. Elasticities and the inverse hyperbolic sine transformation. Oxf. Bull. Econ. Stat. 82 (1), 50–61. https://doi.org/10.1111/obes.12325.

Bickel, P., Friedrich, R., Droste-Franke, B., Bachmann, T., Greßmann, A., Rabl, A., Hunt, A., Markandya, A., Tol, R., Hurley, F., Navrud, S., Hirschberg, S., Burgherr, P., Heck, T., Torfs, R., De Nocker, L., Vermoote, S., Int Panis, L., Tidblad, J., 2005. Extern E Externalities of Energy Methodology 2005 Update. https://www.ier.uni-stuttgart.de/en/research/projects/externe/.

Bivand, R.S., Pebesma, E., Gómez-Rubio, V., 2013. Applied spatial data analysis with R. Use R!. https://doi.org/10.1007/978-1-4614-7618-4.

Borck, R., Schrauth, P., 2021. Population density and urban air quality. Reg. Sci. Urban Econ. 86, 103596. https://doi.org/10.1016/j.regsciurbeco.2020.103596.

Castro Campos, B., Petrick, M., 2023. Nitrogen surplus displays a spurious environmental Kuznets curve in Germany. Ger. J. Agric. Econ. 72 (2), 91–100. https://doi.org/10.22004/AG.ECON.343349.

Cembureau, 2017. The Story of Cement Manufacture. In: https://www.cementeurope.eu/about-us/the-manufacturing-process/.

Chen, J., Zeng, J., Shi, C., Liu, R., Lu, R., Mao, S., Zhang, L., 2019. Associations between short-term exposure to gaseous pollutants and pulmonary heart disease-related mortality among elderly people in Chengdu, China. Environ. Health 18 (1), 64. https://doi.org/10.1186/s12940-019-0500-8.

Dai, Y.H., Zhou, W.X., 2017. Temporal and spatial correlation patterns of air pollutants in Chinese cities. PLoS One 12 (8), e0182724. https://doi.org/10.1371/journal.pone.0182724.

Destek, M.A., Ulucak, R., Dogan, E., 2018. Analyzing the environmental Kuznets curve for the EU countries: the role of ecological footprint. Environ. Sci. Pollut. Res. 25 (29), 29387–29396. https://doi.org/10.1007/s11356-018-2911-4.

Dinda, S., 2004. Environmental Kuznets curve: a survey. Ecol. Econ. 49 (4), 431–455. https://doi.org/10.1016/j.ecolecon.2004.02.011.

Ding, W., Liu, J., 2023. Nonlinear and spatial spillover effects of urbanization on air pollution and ecological resilience in the Yellow River Basin. Environ. Sci. Pollut. Res. 30 (15), 43229–43244. https://doi.org/10.1007/s11356-023-25193-4.

Elhorst, J.P., 2010. Applied spatial econometrics: raising the bar. Spat. Econ. Anal. 5 (1), 9–28. https://doi.org/10.1080/17421770903541772.

European Environment Agency, 2022. Air Quality Data Viewer – Average Concentrations and Health Impact by Country and Region (NUTS). https://discomap.eea.europa.eu/App/AQViewer/index.html.

European Environment Agency, 2023. EMEP/EEA Air Pollutant Emission Inventory Guidebook 2023.2.A.1. Cement Production. https://www.eea.europa.eu/publications/emep-eea-guidebook-2023.

European Environment Agency, 2025. Air Quality Status Report 2025: Nitrogen Dioxide - NO2. https://www.eea.europa.eu/en/analysis/publications/air-quality-status-report-2025/nitrogen-dioxide.

European Environment Agency, 2025a. Air Quality Data Viewer – Average Concentrations and Health Impact by Country and Region (NUTS). https://discomap.eea.europa.eu/App/AQViewer/index.html.

Eurostat, 2025. NUTS - Nomenclature of Territorial Units for Statistics. https://ec.europa.eu/eurostat/en/web/nuts/overview.

Eurostat, 2026. Gross Domestic Product (GDP) at Current Market Prices by NUTS 3 Regions (nama_10r_3gdp). https://doi.org/10.2908/NAMA_10R_3GDP.

Feng, T., Du, H., Lin, Z., Zuo, J., 2020. Spatial spillover effects of environmental regulations on air pollution: evidence from urban agglomerations in China. J. Environ. Manag. 272, 110998. https://doi.org/10.1016/j.jenvman.2020.110998.

Firdissa, B., Degefa, S., Mulugeta, E., Sithole, D., 2024. Emissions from Ethiopian clinker-producing cement factories and their impact on community well-being. Discov. Appl. Sci. 6 (8), 429. https://doi.org/10.1007/s42452-024-06082-y.

German Environment Agency, 2022. German Informative Inventory Report. https://iir.umweltbundesamt.de/2022/sector/ippu/mineral_industry/cement_production/start.

German Environment Agency, 2025. Air Pollutant Emissions. Emissions Overviews 1990–2023 for Air Pollutants. https://www.umweltbundesamt.de/themen/luft/emissionen-von-luftschadstoffen.

Halkos, G., 2011. Environment and Economic Development: Determinants of an EKC Hypothesis. Munich Personal RePEc Archive. https://mpra.ub.uni-muenchen.de/32470/.

Jiang, Y., Niu, Y., Xia, Y., Liu, C., Lin, Z., Wang, W., Ge, Y., 2019. Effects of personal nitrogen dioxide exposure on airway inflammation and lung function. Environ. Res. 177, 108620. https://doi.org/10.1016/j.envres.2019.108620.

Joint Research Center of European Commission, 2025a. AGRI4CAST Data Portal. https://agri4cast.jrc.ec.europa.eu/dataportal.

Joint Research Center of European Commission, 2025b. AGRI4CAST Resources Portal. https://agri4cast.jrc.ec.europa.eu/dataportal.

Kraftfahrt Bundesamt, 2025. Statistikportal. https://das-kba-statistikportal.hub.arcgis.com/search.

LeSage, J., Pace, R.K., 2009. Introduction to Spatial Econometrics. https://doi.org/10.1201/9781420064254.

LeSage, J.P., Pace, R.K., 2014. Interpreting spatial econometric models. In: Handbook of Regional Science, pp. 1535–1552. https://doi.org/10.1007/978-3-642-23430-9_91.

Li, M., Li, C., Zhang, M., 2018. Exploring the spatial spillover effects of industrialization and urbanization factors on pollutants emissions in China's Huang-Huai-Hai region. J. Clean. Prod. 195, 154–162. https://doi.org/10.1016/j.jclepro.2018.05.186.

Li, M., Zhang, M., Du, C., Chen, Y., 2020. Study on the spatial spillover effects of cement production on air pollution in China. Sci. Total Environ. 748, 141421. https://doi.org/10.1016/j.scitotenv.2020.141421.

Ma, Y.R., Ji, Q., Fan, Y., 2016. Spatial linkage analysis of the impact of regional economic activities on PM2.5 pollution in China. J. Clean. Prod. 139, 1157–1167. https://doi.org/10.1016/j.jclepro.2016.08.152.

Moran, P.A., 1950. Notes on continuous stochastic phenomena. Biometrika 37 (1/2), 17–23. https://doi.org/10.2307/2332142.

Nwogu, F.U., Ubuoh, E.A., Kanu, C., Ogbaji, E.E., Nwawuike, N., 2025. Effect of cement production processes on dry atmospheric chemistry in south-South Nigeria. Environ. Sci. Eur. 37 (1), 90. https://doi.org/10.1186/s12302-025-01135-4.

OECD, 2025. Monitoring and Preventing Industrial Pollution - Pollutant Release and Transfer Register. https://www.oecd.org/en/topics/monitoring-and-preventing-industrial-pollution.html.

Radukić, S., Perović, D., 2019. Internalizing environmental externalities in cement industry: case study for the Republic of Serbia and selected neighboring countries. In: Facta Universitatis, Series: Economics and Organization, pp. 379–392. https://doi.org/10.22190/FUEO1804379R.

Rüttenauer, T., 2018. Neighbours matter: a nation-wide small-area assessment of environmental inequality in Germany. Soc. Sci. Res. 70, 198–211. https://doi.org/10.1016/j.ssresearch.2017.11.009.

Salima, B.A., Bellefon, M.D., 2018. Spatial autocorrelation indices (Ch. 3). In: Handbook of Spatial Analysis: Theory and Application with R, pp. 51–68. https://www.insee.fr/en/information/3635545.

Schorcht, F., Kourti, I., Scalet, B.M., Roudier, S., Delgado Sancho, L., 2013. Best Available Techniques (BAT) Reference Document for the Production of Cement, Lime and Magnesium Oxide. https://doi.org/10.2788/12850.

Shekhar, S., Xiong, H., 2007. Encyclopedia of GIS. Springer Science & Business Media, New York.

Shen, Y., Jiang, F., Feng, S., Zheng, Y., Cai, Z., Lyu, X., 2021. Impact of weather and emission changes on NO2 concentrations in China during 2014–2019. Environ. Pollut. 269, 116163. https://doi.org/10.1016/j.envpol.2020.116163.

Sun, A., He, Q., Xiao, C., Hua, Y., Zhang, J., 2024. The spatial spillover effects of regional integration on carbon emissions. Int. Rev. Econ. Financ. 95, 103447. https://doi.org/10.1016/j.iref.2024.103447.

Sustainability Directory, 2024. Atmospheric Dispersion. https://pollution.sustainability-directory.com/term/atmospheric-dispersion/.

Thunis, P., Clappier, A., Tarrason, L., Cuvelier, C., Monteiro, A., Pisoni, E., Wesseling, J., Belis, C.A., Pirovano, G., Janssen, S., Guerreiro, C., Peduzzi, E., 2019. Source apportionment to support air quality planning: strengths and weaknesses of existing approaches. Environ. Int. 130, 104825. https://doi.org/10.1016/j.envint.2019.05.019.

Thürkow, M., Banzhaf, S., Butler, T., Pültz, J., Schaap, M., 2023. Source attribution of nitrogen oxides across Germany: comparing the labelling approach and brute force technique with LOTOS-EUROS. Atmos. Environ. 292, 119412. https://doi.org/10.1016/j.atmosenv.2022.119412.

VDZ, 2023. Environmental Data of the German Cement Industry. https://www.vdz-online.de/fileadmin/wissensportal/publikationen/umweltschutz/Umweltdaten/VDZ_Umweltdaten_Environmental_Data_2023.pdf.

VDZ, 2025. Cement Industry. https://www.vdz-online.de/en/cement-industry/cement-industry.

VDZ (Personal Communication), 2026. Verified Emission Data per Cement Plant and Year, EU Transaction Log. Dataset.

Wærsted, E.G., Sundvor, I., Denby, B.R., Mu, Q., 2022. Quantification of temperature dependence of NOx emissions from road traffic in Norway using air quality modelling and monitoring data. Atmos. Environ. X 13, 100160. https://doi.org/10.1016/j.aeaoa.2022.100160.

Wang, C., Du, X., Liu, Y., 2017. Measuring spatial spillover effects of industrial emissions: a method and case study in Anhui province, China. J. Clean. Prod. 141, 1240–1248. https://doi.org/10.1016/j.jclepro.2016.09.182.

Wrightson, S., Hosking, J., Woodward, A., 2025. Higher population density is associated with worse air quality and related health outcomes in Tāmaki Makaurau. Aust. N. Z. J. Public Health 49 (1), 100213. https://doi.org/10.1016/j.anzjph.2024.100213.

Wu, X., Tian, Z., Kuai, Y., Song, S., Marson, S.M., 2022. Study on spatial correlation of air pollution and control effect of development plan for the city cluster in the Yangtze River Delta. Socio Econ. Plan. Sci. 83, 101213. https://doi.org/10.1016/j.seps.2021.101213.

Zhao, C., Wang, B., 2022. How does new-type urbanization affect air pollution? Empirical evidence based on spatial spillover effect and spatial Durbin model. Environ. Int. 165, 107304. https://doi.org/10.1016/j.envint.2022.107304.

Zhao, H., Cao, X., Ma, T., 2020. A spatial econometric empirical research on the impact of industrial agglomeration on haze pollution in China. Air Qual. Atmos. Health 13 (11), 1305–1312. https://doi.org/10.1007/s11869-020-00884-w.